Geophys. J. Int. (1998) **132**, 471–478

Inverting seismograms of weak events for empirical Green's tensor derivatives

Vladimír Plicka and Jiří Zahradník

Department of Geophysics, Faculty of Mathematics and Physics, Charles University, V Holešovičkách 2, 180 000 *Praha, Czech Republic*

Accepted 1997 February 3. Received 1996 October 10; in original form 1996 January 8

SUMMARY

Given a station and a suite of clustered weak event records whose focal mechanisms are known, empirical Green's tensor spatial derivatives (EGTD) can be calculated, almost free of the source effects. The inversion method solves an overdetermined system of linear algebraic equations in the frequency domain, and a FFT provides the time histories. They represent a least-squares averaged representation of the path between the station and the entire focal zone, including multiple P and S phases, coda waves, etc. The method can be used for modelling earthquakes whose focal mechanisms are quite different from the weak events employed. This is proved here using both synthetic seismograms and earthquake swarm records with variable focal mechanisms. It is expected that the EGTD method can improve strong motion syntheses and source inversions.

Key words: discrete wavenumber method, empirical Green's function, strong ground motion, weak events.

1 INTRODUCTION

Green's functions (or, more properly, tensors) play a key role in any seismic investigation. Although various numerical methods have been developed for their calculation in complex media, including 3-D heterogeneity, attenuation and anisotropy, existing structural data often provide theoretical Green's functions consisting of a few seismic phases only, while complex coda and/or surface waves are lacking. That is why empirical Green's functions (EGF) have attracted attention, mainly in detailed source studies and strong ground motion modelling (Hartzell 1978; Kanamori 1979; Irikura 1983; Ammon, Velasco & Lay 1993; Bernard & Zollo 1994; Tumarkin & Archuleta 1994; Jones & Hough 1995; Cassidy 1995; Frankel 1995; Wajeman *et al.* 1995). The main idea behind EGF is that weak events, because of their small fault extents and short durations, yield information about the complete transfer properties of the medium between a given focal zone and station, with minimal effects from a complex source.

Although basically true, the weak-event records cannot be *directly* used as Green's functions, for at least two reasons: each has a small but finite (and different) source duration, and they do not correspond to single forces but to (different) dislocations. For these reasons, most previous studies employing EGF either assumed similar focal mechanisms, or only approximately corrected for radiation pattern differences between the weak events and the synthesized strong one.

The aim of this paper is to develop a method for calculating empirical Green's tensor spatial derivatives (EGTD) which as much as possible removes the presumably double-couple source effects from the weak-event records employed. The resulting time histories can, thus, be used to synthesize ground motion records for events of an arbitrary source time function and focal mechanism. Path effects are completely described, including body and surface phases and coda waves. Of course, the applicability of the EGTD cannot be extended beyond the source–station pair and the frequency band of the weak-event records.

In fact, our method is related to the well-known inversion for the moment tensor time function, $M_{pq}(t)$. In that inversion the Green's tensor derivatives $G_{ip,q}(t)$ must be known. Conversely, we assume knowledge of the moment tensor, and solve for path effects. This might appear as a logical 'loop': where should $M_{pq}(t)$ be taken from when $G_{ip,q}(t)$ is being determined? Because we deal with *weak* events, the time variation of the moment tensor can be estimated, while its tensorial character (that is the focal mechanism) can be found using simple structural models and a low-frequency theoretical approximation to the Green function only. That is the main trick of the present method.

2 METHOD

Consider a suite of weak events $j = 1, 2, \ldots$ m, whose foci ξ_j belong to a relatively small zone (Fig. 1). Let L denote the characteristic size of the focal zone, and ξ_0 mark a reference point inside. The events are recorded at a station x, where the

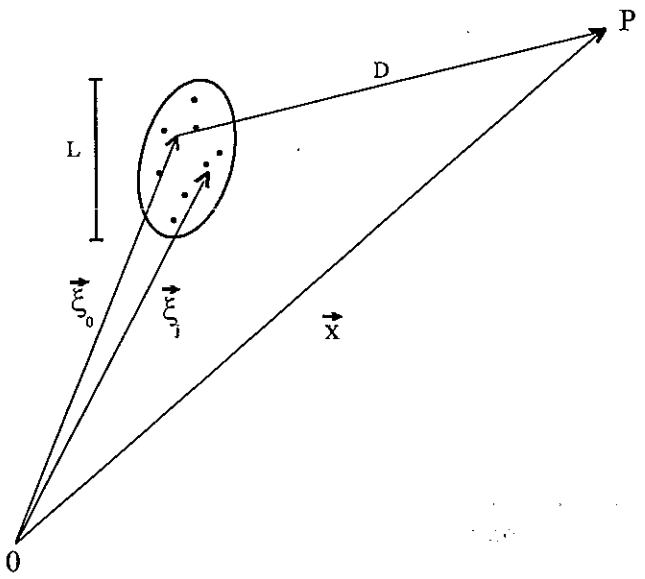

Figure 1. Schematic representation of the weak events and station for which the EGTD are determined.

distance $D = |\mathbf{x} - \xi_0|$ is large compared to L. The events are weak, that is their fault lengths are small compared to D. Then, for wavelengths larger than the fault lengths, the point-source approximation of the displacement components $i = 1, 2, 3$ of the jth event read (Chapter 3.3 of Aki & Richards 1980)

$$u_i^j(\mathbf{x}, t) = M_{pq}^j(\xi_j, t) * G_{ip,q}(\mathbf{x}, \xi_0, t, 0). \quad (1)$$

Here M_{pq}^j is the moment tensor of jth event, $G_{ip,q}$ denotes the Green's tensor spatial derivatives, the asterisk marks the time convolution operator, and Einstein's summation convention over indices $p, q = 1, 2, 3$ is used. The assumption of the spatial proximity of the events has been already used in eq. (1), which is why a single Green's tensor (at ξ_0) appears for an arbitrary j. We are interested in $G_{ip,q}(\mathbf{x}, \xi_0, t, 0)$, describing the 'average' transfer properties of the medium between the station and the entire focal zone, which we call the EGTD. The EGTD are *complete* Green's functions, including all existing body and surface waves (if present) and coda waves.

Now we transform eq. (1) into the frequency domain, and keep the same notation for both the time functions and their spectra: u, M, G. Then, for one component (say $i = 1$), and frequency f, we obtain a simple linear equation:

$$u_1^j(\mathbf{x}, f) = M_k^j(\xi_j, f) G_{1k}(\mathbf{x}, \xi_0, f). \quad (2)$$

Here an abbreviated denotation with one subscript k instead of the two p, q has been used, in which $k = 1, 2, \ldots n$ ($n = 5$ or 6, see below). Collecting such equations for all events we obtain a linear algebraic system relating, at a given frequency, the observed u and the unknown G:

$$\begin{pmatrix} u_1^1 \\ u_1^2 \\ \cdot \\ \cdot \\ \cdot \\ u_1^m \end{pmatrix} \begin{pmatrix} M_1^1 & M_2^1 & \cdot & \cdot & \cdot & M_n^1 \\ M_1^2 & M_2^2 & \cdot & \cdot & \cdot & M_n^2 \\ \cdot & \cdot & \cdot & \cdot & \cdot & \cdot \\ \cdot & \cdot & \cdot & \cdot & \cdot & \cdot \\ \cdot & \cdot & \cdot & \cdot & \cdot & \cdot \\ M_1^m & M_2^m & M_3^m & \cdot & \cdot & M_n^m \end{pmatrix} \begin{pmatrix} G_{11} \\ G_{12} \\ \cdot \\ \cdot \\ \cdot \\ G_{1n} \end{pmatrix}. \quad (3)$$

In the applications discussed below, typical values of $m \approx 10$ have been used. Then $m > n$, the system is overdetermined, hence it is solved in the least-squares sense (Tarantola 1987).

In the following synthetic tests and real-data applications we have used both undamped least squares and damped least squares with different numerical values of the damping factors. When decreasing the damping factors, the results have converged to those from the undamped method. Therefore, all results presented below are from the undamped least squares. We also note that the same numerical results have been obtained when solving eq. (3) directly as a complex-valued system by Gaussian elimination, or solving it as two real-valued systems (for real and imaginary parts) by means of Gaussian elimination with pivoting.

Calculating $G_{11}(f), \ldots G_{1n}(f)$ *repeatedly* for discrete frequencies within a studied band, and transforming back into the time domain by FFT, we obtain the time histories $G_{11}(t), \ldots G_{1n}(t)$. Then, the remaining ground-motion components $i = 2$ and 3, quite independently of each other, will provide $G_{21}(t), \ldots G_{2n}(t)$ and $G_{31}(t), \ldots G_{3n}(t)$.

When dealing with velocity $\dot{u}_i(t)$ instead of the displacement $u_i(t)$, the moment rate function $\dot{M}_{pq}(t)$ appears instead of $M_{pq}(t)$.

Solution of eq. (3) requires that the appropriate moment tensors $M_{pq}(t)$ are known. No major problem arises from the requirement of the time histories $M(t)$, assumed to be the same for all P, q: dealing with weak events, their source time function can be represented by a simple analytic function, for example a smooth step for $M(t)$ (Bouchon 1981), or a triangle or trapezoid for $\dot{M}(t)$. Hence, only the duration of $M(t)$ is needed. This, as a rule, can be fairly well estimated from the corner frequency, or directly read from the displacement records. The required tensorial components of M_{pq}, that is the focal mechanism, impose more difficulties. As the events are weak, recording by a local network is necessary, and some of the amplitude-based methods should be used for the focal mechanism determination (Slunga 1981; Pearce 1987; Saikia & Herrmann 1987; Zhao & Helmberger 1994). Another important requirement is a recording up to low frequencies, because the time-dependent M_{pq} tensor [$M_{pq} = \lim_{t \to \infty} M_{pq}(t)$] is a static quantity, related to the earthquake spectrum in the limit of $f \to 0$. As earthquake displacement spectra are flat below the corner frequency, solving for M_{pq} can be performed at low frequencies, not necessarily just at the zero frequency, hence it is a stable task. Moreover, the lower the considered frequency is, the less detailed the required knowledge of the medium required in the modelling is. Therefore, when searching for the time-independent tensor M_{pq}, relatively simple structural models can be used. (In other words, there is no logical 'loop' in our method, because the required knowledge of M_{pq} relies on the low-frequency approximate Green's function, while our concern is in obtaining empirical Green's functions in the entire frequency band of the weak earthquakes employed.) Under these conditions very few three-component broad-band stations can provide the necessary focal mechanisms using the methods of Langston (1982), Dreger & Helmberger (1993), and Fan & Wallace (1995). We used the focal mechanism determination method of Kolář (1994).

Two parametrizations of M (and correspondingly of G) were tested in this paper. The six-component parametrization in the Cartesian coordinates $i = 1, 2, 3 = x$ (north), y (east), z (down)

is given by $M_1 = M_{xx}$, $M_2 = M_{xy}$, $M_3 = M_{xz}$, $M_4 = M_{yy}$, $M_5 = M_{yz}$, $M_6 = M_{zz}$. See Aki & Richards (1980) eq. (1), box 5.5, p. 117 for an explanation of how these components can be related to strike, dip and rake. The five-component parametrization is as follows (Coutant 1989):

$$M_1 = M_{xy}, \qquad M_2 = M_{xz}, \qquad M_3 = -M_{yz},$$

$$M_4 = \frac{-2M_{xx} + M_{yy} + M_{zz}}{3}, \qquad M_5 = \frac{M_{xx} - 2M_{yy} + M_{zz}}{3}.$$

The latter explicitly expresses the assumption of the vanishing volume change. During our synthetic tests with double-couple events, the five-component parametrization was found to be preferable, because the corresponding EGTD is less affected by numerical noise.

There are several factors limiting the width of the spectral band of the weak-event records, including the finite extent of their fault planes, the attenuation of the medium, and instrumental response. Obviously, it is desirable to solve eq. (3) within the whole available bandwidth. However, numerical problems can arise at frequencies close to its effective end. This is so because solving eq. (3) is, in fact, equivalent to a 'division' by the moment tensor spectrum. Therefore, when inspecting the spectra of the weak events, we first define an artificial cut-off frequency slightly lower than the effective spectral end (that is, the lowest cut-off from the whole suite of the weak events). We then perform the inversion by eq. (3) up to that cut-off only, and finally apply a cosine taper in the frequency domain. The remaining terms of the FFT series, up to the Nyquist frequency, are padded by zeros.

3 VERIFICATION ON SYNTHETIC DATA

Synthetic tests were performed on seismograms that we calculated using the discrete wavenumber (DW) method (Bouchon 1981) combined with the matrix method (Kennett & Kerry 1979). A computer program developed by Coutant (1989) was used. The method provides accurate and complete wavefields, automatically containing all body waves and surface waves, generated by a point source in a given 1-D (horizontally layered) model. Near-field effects are also included.

We considered a layered crustal model representing the seismically active (swarm) region in West Bohemia, Czech Republic (Table 1, Novotný 1983), and a hypothetical station at $x = 6000$ m, $y = 0$ m, $z = 0$ m. In Test 1, the horizontal-component velocity–time histories were calculated for 12 weak events (Table 1). The events were arbitrarily and irregularly distributed inside a focal zone of $x \in (-200, 200)$ m, $y \in (-100, 200)$ m, $z \in (8000, 8500)$ m. Their focal mechanisms were simulated to vary widely with the strike $\Phi \in (15°, 330°)$, dip $\delta \in (5°, 89°)$ and rake $\lambda \in (-120°, 280°)$, while the prescribed source duration ranged from 0.55 to 0.66 s. Assuming a stress drop of 0.1 MPa, this would reflect the variability of the scalar moments from 3.9 to 6.7×10^{14} N m. With an average predominant frequency of 1.7 Hz, the P and S wavelengths at the source depth were $\lambda_P = 3823$ m and $\lambda_S = 2205$ m, respectively. Thus, taking a characteristic length of the focal zone as $L = z_{max} - z_{min} = 500$ m, we obtain $\lambda_P/L = 7.6$ and $\lambda_S/L = 4.4$. The 12 velocity–time histories were inverted for five vertical velocity components of the EGTD in the frequency band $f \in (0, 22)$ Hz, at equal intervals of $\Delta f = 0.1$ Hz, and cosine-tapered between 7.0 and 14.0 Hz. The resulting five-component EGTD (Fig. 2) calculated by FFT on 1024 points consists of relatively simple basic wave groups only. It is almost free of any numerical noise, except the low-amplitude oscillations due to the necessary frequency filtering mentioned at the end of the preceding section.

Table 1. The crustal model used in the synthetic tests.

Layer No.	Thickness (km)	α (km s^{-1})	β (km s^{-1})	ρ (kg m^{-3})
1	1	5.6	3.23	2820
2	1	5.8	3.35	2860
3	2	6.0	3.46	2900
4	26	6.5	3.75	3000

Solving the overdetermined 12×5 system (eq. 3) yields an EGTD which does not automatically return the original weak-motion records when 'back-substituted' into eq. (3) and convolved with their moment tensors. However, comparing such EGTD-based synthetics with the original ones provides a useful verification of our method. Typical comparisons, selected to represent the best, intermediate and worst fits, are shown in Fig. 3. The overall agreement is good, while the partial misfits can be explained by differences between the true Green's functions of the individual events and their approximation that 'averages' the entire focal zone. Also contributing to the observed misfit is the variability of the source durations and focal mechanisms which, while inverting (eq. 3), is accounted for in the least-squares sense only. The latter has been proved (but not shown here) by an experiment in which slight disagreements persisted even in the case when all weak events had exactly the same hypocentral location.

Two more tests (not shown here) were performed to see how the result depends on the size of the focal zone. Test 2 used 12 events regularly distributed in the nodes of the fully horizontal focal area of 300×200 m, that is in a smaller zone than in Test 1. At the same time, shorter source durations compared to Test 1 were used. This experiment, characterized by $\lambda_P/L = 2.2$, $\lambda_S/L = 1.25$ resulted in a worse agreement than in Fig. 3, mainly in the S-wave group. Test 3 used the same foci as Test 2, but the source durations were enlarged to give $\lambda_P/L = 8.7$, $\lambda_S/L = 5.0$. This case resulted in a very good fit, even better than in Fig. 3. The tests proved that the quality of the EGTD increases when the size of the weak-event focal zone (measured with respect to wavelength) decreases.

To verify further the result of Test 1 (Fig. 2), we convolved it with the moment tensor time function of an event *not used* during the EGTD inversion. The hypocentre ($x = -50$ m, $y = 100$ m, $z = 8400$ m) was assumed inside the previously investigated focal volume, but its focal mechanism ($\Phi = 50°$, $\delta = 89°$, $\lambda = 125°$) did not equal any of the weak events employed. The source duration, $T = 0.8$ s, was chosen to be considerably larger to model a stronger earthquake. A good agreement between the EGTD-based synthetic record, and that directly calculated by the DW method has been found (Fig. 4).

4 APPLICATION TO EARTHQUAKE DATA

The method has been applied to the earthquake swarm in West Bohemia, Czech Republic. During the period December

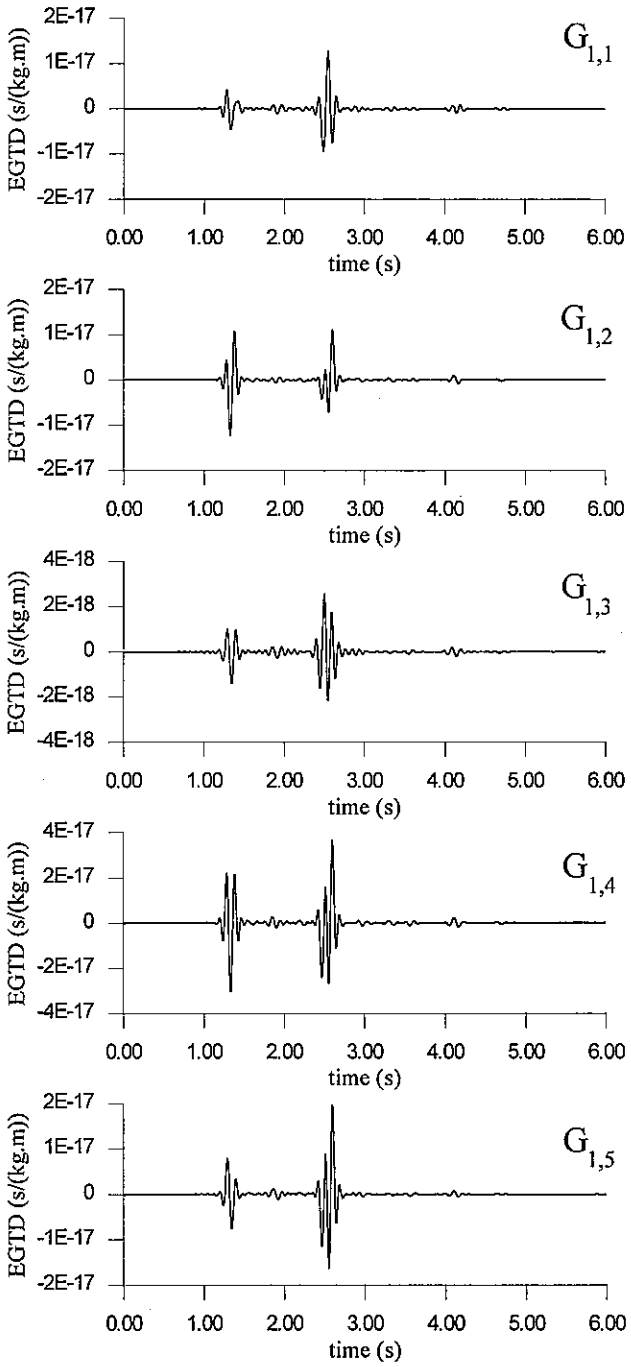

Figure 2. Five vertical components of the EGTD determinated from the *synthetic* weak events of Test 1.

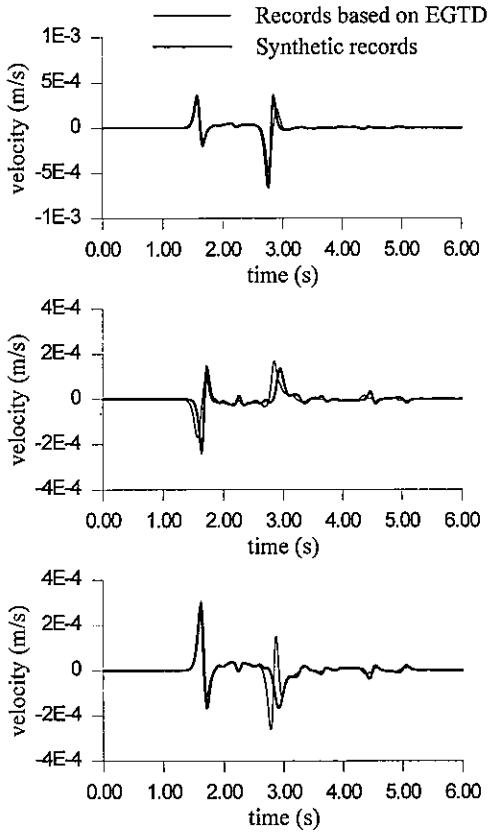

Figure 3. The comparison between the selected original synthetic weak-event records (heavy lines) and the records obtained from the EGTD of Fig. 2 (thin lines).

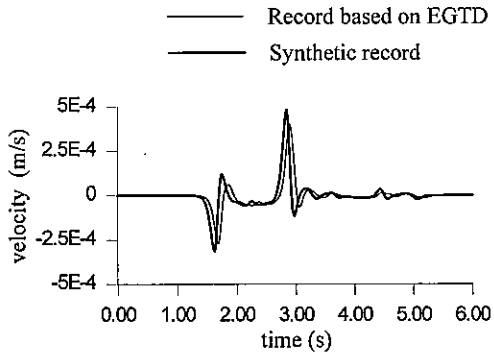

Figure 4. The comparison between the synthetic record *not included* in the EGTD determination (heavy line), and the record obtained from the EGTD of Fig. 2 (thin line).

1985–April 1986, more than 1000 events with local magnitudes ranging from 0.7 to 4.2 were digitally recorded in that area (Kárník, Schenková & Schenk 1987). In this paper velocity records from the three-component temporary station Vackov (VAC; 50.235°N, 12.379°E) are used, recorded with a constant magnification in a frequency band from 0.6 to 30 Hz (Horálek & Jedlička 1987). Only vertical components are analysed here, consisting of 640 samples with a sampling interval of 7 ms, cosine tapered at the ends of the records and low-pass filtered to remove the 50 Hz electric noise. Examples of the velocity record, its Fourier amplitude spectrum, the displacement integrated from the velocity and its log–log spectrum are given in Fig. 5.

More than 143 events of the swarm were previously analysed in great detail by Kolář & Vavryčuk (1990) and Kolář (1992). Thus, well-determined locations, scalar seismic moments and also the amplitude-constrained double-couple focal mechanisms (Kolář 1994), and radiated energies are available. Selected for the present work were 10 of these events ($M_0 \approx 10^{10} - 10^{12}$ N m, Table 2), with foci distributed in a relatively narrow zone of $x \in (5420, 5850)$ m, $y \in (-670, -280)$ m, $z \in (8270, 8860)$ m, while the origin of the x (north), y (east), z (down) coordinate

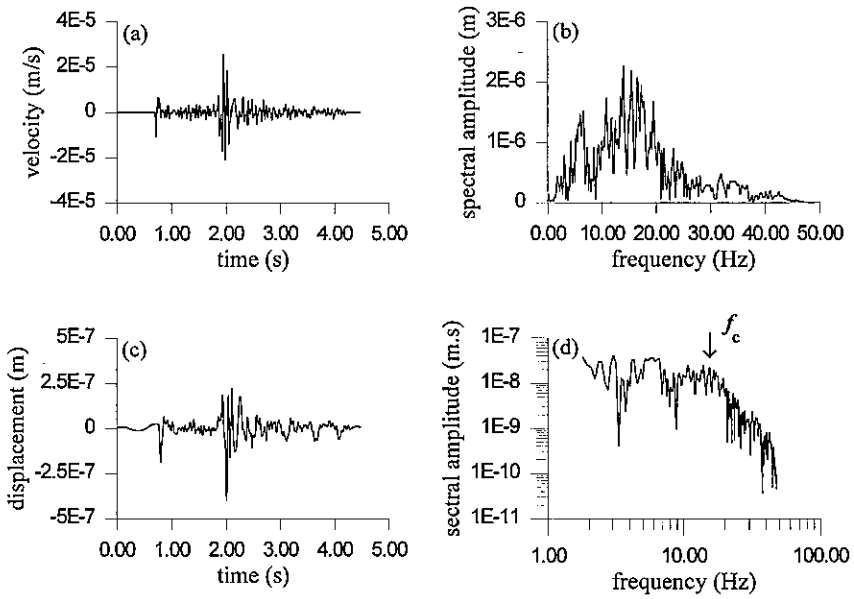

Figure 5. An example of the weak event used in this study (number 10 of Table 2). (a) Velocity record; (b) amplitude spectrum of the velocity record; (c) displacement integrated from the velocity record; (d) log–log spectrum of the displacement record. Also marked is the corner frequency f_c.

Table 2. The focal parameters of the West Bohemia weak earthquakes.

Event No.	M_0 (N m)	M_L	Φ (°)	δ (°)	λ (°)	x (km)	y (km)	z (km)	T (s)	f_c (Hz)
1	8.15×10^{10}	0.87	215	73	−56	5.44	−0.29	8.68	0.035	19
2	2.11×10^{11}	1.01	232	86	−53	5.85	−0.59	8.56	0.048	14
3	1.68×10^{12}	1.41	238	89	−8	5.73	−0.47	8.67	0.051	13
4	8.55×10^{11}	1.37	219	89	−3	5.42	−0.48	8.83	0.042	16
5	3.00×10^{12}	1.69	203	84	−28	5.69	−0.59	8.35	0.039	17
6	3.68×10^{11}	1.17	208	90	3	5.59	−0.51	8.35	0.051	13
7	2.02×10^{12}	1.83	222	84	−15	5.54	−0.28	8.86	0.051	13
8	5.17×10^{12}	2.15	193	90	−2	5.43	−0.54	8.56	0.039	17
9	2.20×10^{11}	1.01	187	90	−28	5.47	−0.67	8.54	0.037	18
10	8.33×10^{11}	1.36	177	88	−16	5.61	−0.44	8.27	0.048	14

system was at the station VAC (Fig. 6a). Their local magnitudes, M_L, ranged from 0.87 to 2.15 (Neunhöfer *et al.* 1989, Table 2). Nine of the events (number 8 was excluded) were used for the EGTD determination, with number 8 used later for verification. The inversion was performed from 0 to 49 Hz at equal intervals of $\Delta f = 0.1395$, padded by zeros to 1024 complex points. The entire computation, including the inverse FFT, took about 3 s on a HP-735 workstation. Taking $L = z_{max} - z_{min} = 510$ m and an average corner frequency of 15.2 Hz, the ratios $\lambda_P/L \approx 0.74$, $\lambda_S/L \approx 0.43$ were estimated at the source depth. Compared to the synthetic tests, these are rather low, implying that a single EGTD only approximates the entire focal zone.

Because the focal mechanisms were available (Table 2), and the moment function time variation was assumed to be a smooth step again, the only parameters left for estimation were the source durations T. These were determined from the corner frequencies f_c (Table 2 and the example given in Fig. 5).

The corresponding time histories of the vertical components $G_{31}, G_{32}, \ldots G_{35}$ are shown in Fig. 6(b). These functions reveal complexity in both P- and S-wave groups and their codas. None of the existing crustal models of the area (for example that of Table 1) provides such a detailed path representation as the present method. Compare, for example, the simple synthetics shown in Figs 2–4. In this sense, the calculated EGTD can contribute to future refinements of the crustal structure in the area studied.

To validate the time histories of EGTD, we convolved them with the moment tensors of the weak events previously used during the inversion and compared the results with the original weak-event records. Selected comparisons, representing very good, intermediate, and poor agreement are shown in Fig. 7. We observe a generally worse agreement compared to the synthetic tests because the λ_p/L, λ_s/L ratios are relatively low.

Now a major question remains to be answered: is the method able to synthesize an event *not included* in the inversion? To test this, the true record of event number 8 (Table 2) was compared with the EGTD-based calculated record. As seen from Fig. 8, all of the basic features of the P- and S-wave groups were fitted well, including the absolute amplitudes, the overall envelope shape and the coda duration.

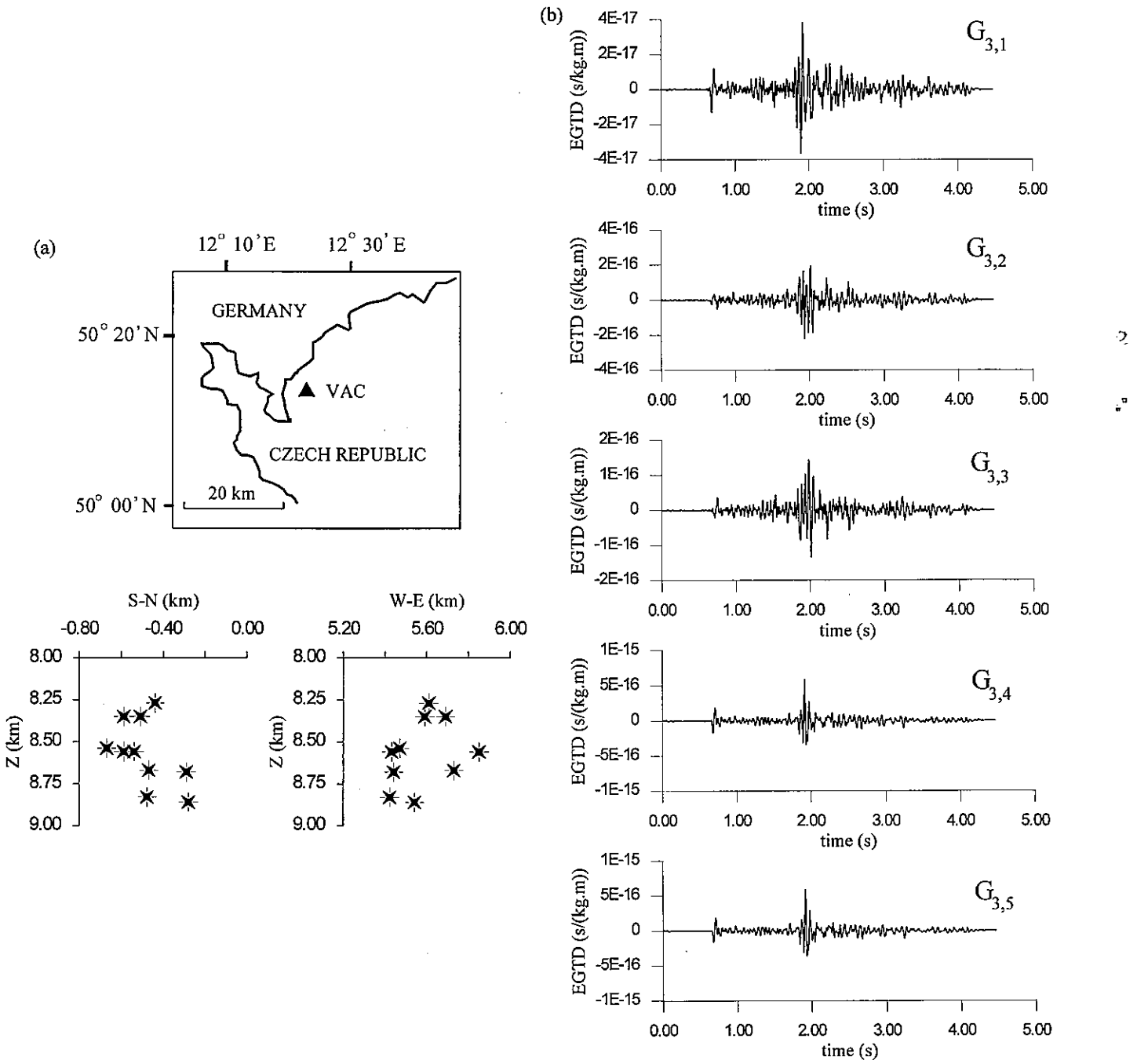

Figure 6. (a) Schematic representation of the West Bohemia region with station VAC and the spatial distribution of weak events (Table 2) in two vertical cross-sections. (b) Five vertical components of the EGTD determined from *real* weak events of Table 2 (except number 8 of Table 2).

These results provide encouragement for modelling the ground motions due to the largest possible events of West Bohemia ($M_0 = 2.66 \times 10^{14}$ N m). Such a step, of course, cannot be realised within the point-source approximation. The EGTD determination should be *repeatedly* performed for several small focal zones like those analysed in this paper, followed by interpolation, and finally subjected to lagged summation according to various rupture-propagation models. Our method seems particularly useful for such modelling because, in the complex tectonic environment of the West Bohemia region, the focal mechanisms of the weak and stronger events can be rather dissimilar.

5 CONCLUSIONS

An inversion method is proposed for the determination of empirical Green's tensor spatial derivatives, EGTD, representing an extension of the classical method of empirical Green's functions, EGF. The method is based on solving an overdetermined linear algebraic system whose data are represented by weak-event records at a station, and the matrix consists of their moment tensor time functions.

Using events of a small size is essential, not only for consistency with the theory (that is the point-source approximation), but also for an easy representation of the moment tensor time

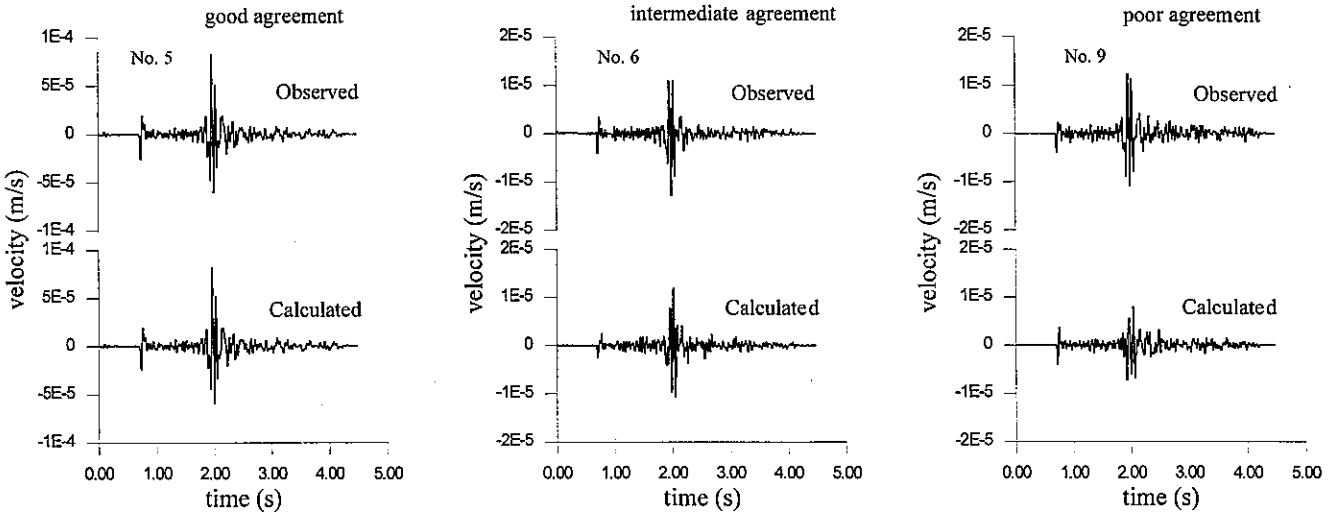

Figure 7. Comparison between the real weak-motion records, used to infer the EGTD (top), and the records obtained from the EGTD of Fig. 6(b) (bottom).

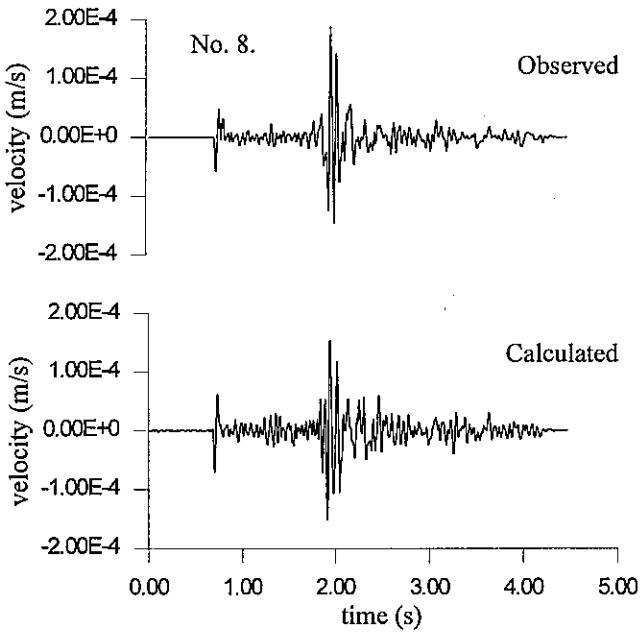

Figure 8. The comparison between the real weak-motion record number 8 (top) *not included* in the EGTD determination and the record obtained from the EGTD of Fig. 6(b) (bottom).

history by a simple analytic function and for easy estimation of the source durations from the records.

Equally essential is the distribution of the events within a focal zone as small as possible (with respect to the wavelength), because the resulting EGTD represents a least-squares averaged transfer function for propagation between the station and the entire focal zone. The smaller the zone, the better the physical meaning of such an averaging, and hence the better the agreement with the actual Green's functions of the individual weak events.

It is appealing both for structural studies and for ground-motion syntheses that the results include many realistic details, which are lacking (as a rule) in theoretical Green's functions based on the current crustal models.

As they are almost free of the focal mechanism effect, the EGTD can be used to synthesize ground motions due to arbitrary events occurring within the same focal zone, and observed at the same station. The durations and focal mechanisms of the events to be modelled, independent of those employed in the inversion, can then be fully taken into account. This useful property was proved on both synthetic and real data (Figs 4 and 8, respectively).

Obviously, if several focal zones, close to the expected fault plane of a major event, are available, the present inversion can be repeatedly performed to obtain the path effects of subevents. These, together with various assumed time functions and focal mechanisms of the subevents (different from each other in general) and assumed rupture-propagation models, can be used for synthesizing strong ground motions. In this sense the EGTD method represents a useful improvement compared to the traditional EGF methods in which the source parameters of the subevents are fixed by the weak events used and cannot be arbitrarily adjusted. For example, with our method, the rise time and the final slip of the individual subevents can vary spatially at a fault plane according to a quasi-dynamic model. This would allow the combination of an empirical path description and a crack-like source simulation. Allowing for an adjustable, spatially varying focal mechanism, segmented and non-planar fault surfaces can also be studied. The method seems to be equally advantageous for the source inversion problems, too.

The Fortran77 computer code EMPIRE, based on the EGTD method, is available upon request from the E-mail address vp@karel.troja.mff.cuni.cz.

ACKNOWLEDGMENTS

The authors thank O. Coutant for his DW code and J. Horálek for the digital earthquake records. O. Novotný, Z. Martinec and O. Čadek suggested the numerical algorithms for solving eq. (3). The constructive criticism and advice of L. E. Jones, V. Vavryčuk and J. Šílený have considerably improved the presentation. A. Vesnaver and P. Carrion stimulated our more detailed experiments with the damped and undamped inversion.

This research has been financially supported by Charles University grant No. 321, Czech Republic grants No. 0507 and 205/96/1743, NATO ENVIR. LG 940714 grant, and NATO Science for Stability GR-Coal grant.

REFERENCES

Aki, K. & Richards, P.G., 1980. *Quantitative Seismology: Theory and Methods,* W. H. Freeman, San Francisco, CA.

Ammon, C.J., Velasco, A.A. & Lay, T., 1993. Rapid estimation of rupture directivity: application to the 1992 Landers ($M_S = 7.4$) and Cape Mendocino ($M_S = 7.2$) California earthquakes, *Geophys. Res. Lett.,* **20,** 97–100.

Bernard, P. & Zollo, A., 1994. The Irpinia (Italy) 1980 earthquake: Detailed analysis of a complex normal faulting, *J. geophys. Res.,* **94,** 1631–1647.

Bouchon, M., 1981. A simple method to calculate Green's functions for elastic layered media, *Bull. seism. Soc. Am.,* **71,** 959–971.

Cassidy, J.F., 1995. Rupture directivity and slip distribution for the M_S 6.8 earthquake of 6 April 1992, offshore British Columbia: An application of the empirical Green's function method using surface waves, *Bull. seism. Soc. Am.,* **85,** 736–746.

Coutant, O., 1989. Programme de simulation numerique AXITRA, *Rapport LGIT,* Universite Joseph Fourier, Grenoble.

Dreger, D.S. & Helmberger, D.V., 1993. Determination of source parameters at regional distances with three-component sparse network data, *J. geophys. Res.,* **98,** 8107–8125.

Fan, G. & Wallace, T., 1995. Focal mechanism of a recent event in South Africa: A study using a sparse very broadband network, *Seism. Res. Lett.,* **66,** 13–18.

Frankel, A., 1995. Simulating strong motions of large earthquakes using recordings of small earthquakes: the Loma Prieta mainshock as a test case, *Bull. seism. Soc. Am.,* **85,** 1144–1160.

Hartzell, S.H., 1978. Earthquake aftershocks as Green's functions, *Geophys. Res. Lett.,* **5,** 1–4.

Horálek, J. & Jedlička, P., 1987. Temporary three component digital seismic stations Vackov and Nový Kostel, in *Earthquake Swarm 1985/86 in Western Bohemia,* pp. 132–141, ed. Procházková, D., Geophysical Institute, Czechoslovak Academy of Sciences, Praha.

Irikura, K., 1983. Semi-empirical estimation of strong ground motions during large earthquakes, *Bull. Disaster Prev. Res. Inst., Kyoto Univ.,* **33,** 63–104.

Jones, L.E. & Hough, S.E., 1995. Analysis of broadband records from the 28 June 1992 Big Bear earthquake: Evidence of a multiple-event source, *Bull. seism. Soc. Am.,* **85,** 688–704.

Kanamori, H., 1979. A semi-empirical approach to prediction of long-period ground motions from great earthquakes, *Bull. seism. Soc. Am.,* **69,** 1645–1670.

Kárník, V., Schenková, Z. & Schenk, V., 1987. Time pattern of the swarm of December 1985–March 1986 in West Bohemia, in *Earthquake Swarm 1985/86 in Western Bohemia,* pp. 328–342, ed. Procházková, D., Geophysical Institute, Czechoslovak Academy of Sciences, Praha.

Kennett, B.L.N. & Kerry, N.J., 1979. Seismic waves in a stratified half space, *Geophys. J. R. astr. Soc.,* **57,** 557–583.

Kolář, P., 1992. Energy of the seismic waves, *PhD thesis,* Geophysical Institute, Czechoslovak Academy of Sciences, Praha (in Czech).

Kolář, P., 1994. Simultaneous determination of the source mechanism and the seismic wave energy, *Pageoph,* **143,** 655–671.

Kolář, P. & Vavryčuk, V., 1990. *Reinterpretation of selected events of earthquake swarm 1985/86 in Western Bohemia,* Geophysical Institute, Czechoslovak Academy of Sciences (in Czech).

Langston, C.A., 1982. Single station fault plane solutions, *Bull. seism. Soc. Am.,* **72,** 729–744.

Neunhöfer, H. & Procházková, D., eds, 1989. Earthquake swarm 1985/1986 in Western Bohemia, in *Joint Bull. Local seism. Stations,* Geophysical Institute, Czechoslovak Academy of Sciences, Praha (in Czech).

Novotný, O., 1983. Theoretical dispersion curves for the seismic profile Kašperské Hory (Czechoslovakia)–Ksiaz (Poland), *Studia Geophys. Geod.,* **27,** 157–163.

Pearce, R.G., 1987. The relative amplitude method applied to 19 March 1984 Uzbekistan earthquake and its aftershocks, *Phys. Earth. planet. Inter.,* **47,** 137–149.

Saikia, Ch.K. & Herrmann, R., 1987. Determination of focal mechanism solutions for four earthquakes from Monticello, South Carolina, and crustal structure by waveform modelling, *Geophys. J. R. astr. Soc.,* **90,** 669–691.

Slunga, R., 1981. Earthquake source mechanism determination by use of body-wave amplitudes—an application to Swedish earthquakes, *Bull. seism. Soc. Am.,* **71,** 25–35.

Tarantola, A., 1987. *Inverse Problem Theory,* Elsevier Science, Amsterdam.

Tumarkin, A.G. & Archuleta, R.J., 1994. Empirical ground motion prediction, in *Ann. Geofis. Earthquake Source Mechanics,* eds Bonafede, M. & Cocco, M., **XXXVII,** 1691–1720.

Wajeman, C., Bard, P.-Y., Hatzfeld, D., Diagourtas, D., Makropoulos, K. & Gariel, J.-Ch., 1995. Experimental tests on the empirical Green's function method, in *Proc. 5th Int. Conference on Seismic Zonation, October 17–19, 1995,* pp. 1181–1188. Nice, France, II.

Zhao, L.-S. & Helmberger, D.V., 1994. Source estimation from broadband regional seismograms, *Bull. seism. Soc. Am.,* **84,** 91–104.